ELSEVIER

Journal of Marine Systems 28 (2001) 183–201

JOURNAL OF MARINE SYSTEMS

www.elsevier.nl/locate/jmarsys

Mixing analysis of nutrients, oxygen and inorganic carbon in the Canary Islands region

Fiz F. Pérez [a,*], Ludger Mintrop [b], Octavio Llinás [c], Melchor Glez-Dávila [d], Carmen G. Castro [a], Marta Alvarez [a], Arne Körtzinger [b], Magdalena Santana-Casiano [d], M.J. Rueda [c], Aida F. Ríos [a]

[a] *Consejo Superior de Inv. Cientificas, Instituto de Investigacións Mariñas de Vigo (CSIC), Eduardo Cabello 6, Vigo 36208, Spain*
[b] *Abteilung Meereschemie, Institut für Meereskunde an der Universität Kiel, Düsternbrooker Weg 20, Kiel 24105, Germany*
[c] *Instituto Canario de Ciencias Marinas, Aptdo. 56, TELDE Grand Canary 35200, Spain*
[d] *Departamento de Quimica, Universidad de Las Palmas de Gran Canaria, Campus de Tafira, Las Palmas 35017, Spain*

Received 10 December 1999; accepted 20 December 2000

Abstract

We show the distribution of nutrients, oxygen, total dissolved inorganic carbon (C_T) and total alkalinity (A_T) along three sections close to the Canary Islands, between 18°W and the African coast during Meteor 37/2 cruise (January 1997). From the thermohaline properties of Eastern North Atlantic Central Water (ENACW), Mediterranean Water (MW), Antarctic Intermediate Water (AAIW) and North Atlantic Deep Water (NADW), a mixing model has been established based on the water mass description. It can explain most of the variabilities found in the distribution of the chemical variables, including the carbon system, and it is validated through the use of conservative chemical variables like 'NO.' From nutrients, oxygen, A_T and C_T, the chemical characterisation of the water masses was performed by calculating the concentration of these variables in the previously defined thermohaline end-members. The relative variation of nutrient concentrations, resulting from the regeneration of organic matter, was estimated. Close to the African shelf-break, a poleward undercurrent conveying as much as a 11% of AAIW was observed only in the southern section (28.5°N). From the chemical and thermohaline properties of the end-members, a comparison with data from other oceanic regions was made in respect to conservative chemical variables ('NO'). In addition, a north–south gradient in the ventilation pattern of water masses is observed from the residuals of the model.

Keywords: Water masses; CO_2; Oxygen; Nutrients; 'NO'; 'NCO'; North Atlantic

1. Introduction

Under the framework of the multidisciplinary European project CANIGO (Canary Islands Azores Gibraltar Observations), the oceanographic cruise Meteor 37/2 was conducted on January 1997. The main objectives of this project were to investigate and model the circulation of the water masses in Subtropical Eastern North Atlantic and determine the fluxes of the different biogeochemical variables in this region.

The area north of the Canary Islands and south of Madeira Island (Fig. 1) is characterised in the upper

* Corresponding author. Fax: +34-86-23-19-30.
E-mail address: fiz@iim.csic.es (F.F. Pérez).

0924-7963/01/$ - see front matter
PII: S0924-7963(01)00003-3

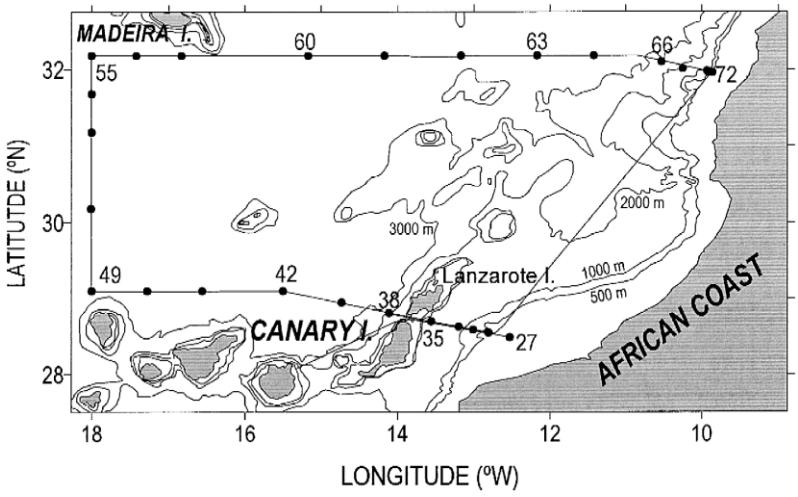

Fig. 1. Location of stations of the MET37/2 cruise (●).

layers by recirculating branches of the North Atlantic's Subtropical Gyre that feed the Canary Current and that are influenced by upwelling events off the African coast (Stramma and Müller, 1989). The region encompasses the eastern boundary current system. The flow field, the water mass transports and the associated biogeochemical fluxes in the region are strongly influenced by (i) the recirculation of the subtropical gyre that feeds the Canary Current, and (ii) the seasonally varying trade wind field with its impact on the upwelling system and the eastern boundary current system off North West Africa.

The thermohaline properties of water masses involved in the Eastern North Atlantic had been extensively described in previous studies (Harvey, 1982; McCartney and Talley, 1982; Fiúza, 1984; Käse et al., 1986; Pollard and Pu, 1985; Ríos et al., 1992; Arhan et al., 1994). In the upper ocean of the Azores region, two varieties of Eastern North Atlantic Central Water (ENACW) (Harvey, 1982; McCartney and Talley, 1982; Ríos et al., 1992)—ENACWt (Eastern North Atlantic Water of subtropical origin) and ENACWp (Eastern North Atlantic Water of subpolar origin)—are involved at different isopycnal levels. At deeper levels, the characteristic salinity minimum of AAIW formed at the Subantarctic Front is detected northward up to 20°N (Reid, 1994). The salinity minimum ($S < 35.4$) detected by Ríos et al. (1992) at 24°N and 22°W can be ascribed to the influence of AAIW according to Willenbrink (1982). Tsuchiya (1989) suggested further northward penetration, up to 47°N, of AAIW traced by a maximum of silicate. However, this maximum could also be due to biogeochemical processes in the water column. In this sense, below the ENACW, the penetration and the influence of Mediterranean Water (MW) are prevalent down to 2000 m in the North Atlantic (Reid, 1994). Below MW, Käse et al. (1986) reported the influence of Labrador Sea Water (LSW). The LSW reaches the African coast after a long excursion along a cyclonic gyre (33–47°N) and a substantial mixing with MW (Reid, 1994; Paillet et al., 1998). Below LSW, the presence of North Atlantic Deep Water (NADW) is detected by the small variability and linearity in the thermohaline structure and the high silicate content (Arhan et al., 1994; Castro et al., 1998). The strong vertical gradient in silicate concentration is due to the downward increasing influence of Antarctic Bottom Water (Stoll et al., 1996). Harvey and Arhan (1988) and Rhein and Hinrichsen (1993) suggest the mixing of NADW and MW. Broecker and Takahashi (1980), Le Groupe Tourbillon (1983) and Kawase and Sarmiento (1986) also point out the possibility of enhanced mixing by a salt-fingering mechanism.

Here we combined the thermohaline and chemical properties to study the chemical variability of the water masses in the Subtropical Eastern North At-

lantic, with specially emphasis on the ventilation and aging pattern. From the water masses variability followed from the thermohaline distribution, several mixing models can been used to quantify the variability of both nutrients and oxygen. One of the most widely used techniques is that of working along isopycnic layers assuming only the existence of lateral mixing (Takahashi et al., 1985; Kawase and Sarmiento, 1986). However, in areas of subduction or upwelling, the vertical advection excludes to allow for any restriction in the modelling of nutrients (Broenkow, 1965; Minas et al., 1982). Tomczak (1981) developed the analysis of sea water masses from mixing triangles without assumption of isopycnal mixing. This kind of analysis can only resolve mixing from three end-members, considering that only salinity and temperature will be used as conservative variables, as has been recently shown for the North Atlantic (Pérez et al., 1993, 1998; Castro et al., 1998). Each of the three water mass end-member is defined by a single and fixed temperature and salinity, while a water mass is conventionally characterised by the mixing of only two end-members, therefore showing a rather fixed TS relationship.

In general, dissolved oxygen and nutrient distributions do not behave in a conservative way due to biological activity. However, it is possible to remove the effect of these processes by knowing the average chemical relations. Broecker (1974) brought forward the concept of 'NO' ('NO' $= R_N NO_3 + O_2$), a conservative tracer which balances the effect of nutrient regeneration by the associated oxygen consumption. His proposed R_N $(= -\Delta O_2{:}\Delta NO_3)$ factor was 9, but a set of different values has been reported in the literature proposed by others, varying between 9 and 10.5 (Redfield et al., 1963; Takahashi et al., 1985; Minster and Boulahdid, 1987; Ríos et al., 1989; Pérez et al., 1993). However, 9.33 was the value most frequently derived by different procedures and from various data sets (Minster and Boulahdid, 1987; Anderson, 1995; Fraga et al., 1998) and it is in agreement with the average chemical composition of phytoplankton (Fraga and Pérez, 1990; Laws, 1991). The regeneration of organic matter also increases the total inorganic carbon (C_T), and thus a similar conservative tracer can be defined ('CO') using the stoichiometric ratio R_C $(= \Delta O_2{:}\Delta C_T)$ which varies in a range from 1.05 to 1.58 (Fraga et al., 1998).

Several multiparametrical models, assuming a conservative behaviour for nutrient, have been used to resolve mixing of more than three end-members (Mackas et al., 1987; Tomczak and Large, 1989). In multivariate analyses, where both conservative (S, θ, 'NO') and non-conservative variables (nutrients, oxygen, C_T and A_T) are handled in the same way, it cannot be discerned which part of the nutrient content is due to remineralization or ventilation processes. In this sense, any variability in the non-conservative tracer could lead to an incorrect definition of new water mass types in areas of very intense biological activity. Alternatively, if the profile of water masses is completely well defined by the thermohaline variability, it is possible to define a mixing model based on a set of vertically ordered mixing triangles. This mixing model can be tested with other conservative tracer as 'NO.' Using the observed non-conservative chemical variables, this model allows the chemical characterisation of the water masses involved and the description of the ventilation and remineralization patterns (Pérez et al., 1993, 1998; Castro et al., 1998).

In this work, a mixing model was developed based on different water masses and their temperature and salinity distribution. The model explains most of chemical variabilities (nutrient, oxygen, alkalinity and C_T) of the water masses. This was tested by application of the conservative chemical tracers. The model residuals allow us to describe the ventilation/aging pattern of the water masses in the study area. The chemical characterisation, including the carbon system, of the water masses will be done and an extensive comparison with other previous chemical characterisation of the water masses in the European basin of the North Atlantic will be shown. Special emphasis will be paid in the spreading of AAIW in order to quantify and clarify the actual importance of the AAIW in the basin.

2. Materials and methods

During FS METEOR cruise 37, leg 2a (January 7–20, 1997), a hydrographic box (CANIGO box) was sampled north–west of the African coast. The box basically consists of three CTD/rosette sections:

the first ran almost zonally from the African coast to a position north of La Palma Island at 29°10′N, 18°00′W; the second went meridionally towards Madeira Island until 32°15′N; and the third then zonally towards the shelf until the 100-m bottom line was reached (Fig. 1). A total of 26 biogeochemical stations were completed on these three sections. Each station consisted of two CTD/rosette—24 bottles cast (shallow and bottom deep) with discrete sampling for dissolved oxygen, nutrients, chlorophyll, pH and several samples for alkalinity (A_T) and total inorganic carbon (C_T) at selected depths: 10, 25, 50, 75, 100, 125, 150, 200, 250, 300, 350, 400, 500, 600, 700, 800,1000, 1100, 1250 and every 250 m to the bottom, including one 20 m above the seafloor.

A Neil Brown MKIIIB CTD was used to obtain continuous profiles of temperature and salinity. The CTD's pressure and temperature sensors were calibrated in the laboratory against WOCE standards. The conductivity sensor was calibrated by comparison with the in situ conductivity of bottle samples taken during the upward profile with the rosette. CTD data processing and removal of typical non-linear effects in sensor responses were performed following Müller et al. (1995). The salinity samples were analysed with a Guildline AUTOSAL salinometer with an accuracy better than 0.002 for single samples.

Dissolved oxygen was measured using an automated potentiometric modification of the original Winkler method following WOCE standards (WOCE, 1994). The standard error for five replicates was less than 2 μmol kg^{-1} (Llinás et al., 1997). The Apparent Oxygen Utilisation (AOU) defined as the deficit of oxygen concentration relative to the atmospheric saturation (UNESCO, 1986) is used to describe the oxygen distribution. Samples for nutrient analysis were frozen at −20°C and then analysed at the ICCM also following WOCE standards (WOCE, 1994). Nutrients were determined by colorimetric methods, using a Technicon AutoAnalyzer AAII. For silicates, a modified Hansen and Grasshoff (1983) method was used, in which β-silicomolybdenic acid is reduced with ascorbic acid. Nitrate was determined after reduction to nitrite in a Cd–Cu column. The standard deviation for duplicates was 0.07 μmol kg^{-1} for silicate, 0.06 μmol kg^{-1} for nitrate and 0.01 μmol kg^{-1} for phosphate. This is equivalent to 0.3%, 0.5% and 0.8% at full scale, respectively.

A coulometric titration technique was used for determining C_T (SOMMA system; Johnson et al., 1993; DOE, 1994). The SOMMA was calibrated with pure CO_2 and tested by running different batches of Certified Reference Material (CRM; provided by A. Dickson, SIO, La Jolla, CA, USA). The precision (between-bottle reproducibility) as judged from regular measurements of duplicate samples was 0.5 μmol kg^{-1}. Accuracy of the data has been estimated to be about 1.5 μmol kg^{-1}.

A Ross Orion 81-04 electrode (Orion Research, Boston, MA, USA) calibrated with 7.413 NBS buffer was used to determine pH (NBS scale). The temperature was measured by a Pt-100 probe. All pH values refer to 15°C to avoid the temperature effect of pH (Pérez and Fraga, 1987). The same CRMs used for C_T determinations were also used to monitor pH measurements. Parallel measurements of pH_{SWS} at 25°C yielded very good agreement with an average deviation of (0.002 ± 0.007) and a high correlation ($r^2 = 0.99$). All pH data were transformed into the SWS scale (pH_{SWS}).

The determination of alkalinity by closed cell titration was performed with two separate potentiometric systems in parallel. The titration systems consist of two titrator type Titrino 702 SM and 719 S (Metrohm, Herisau, Switzerland), respectively: The electrodes used were a Ross glass pH electrode and a double junction silver/silver chloride reference electrode (Orion Research). The acid in a water-jacketed burette and the seawater sample in a water-jacketed cell were maintained at 25 ± 0.1°C using a constant temperature bath. The titration was performed by stepwise adding HCl to the seawater past the carbonic acid end point. A full titration takes about 20 min. The HCl solution (25 l, 0.25 M) was made up from concentrated analytical grade HCl (Merck, Darmstadt, Germany) in 0.45 M NaCl, in order to yield an ionic strength similar to open ocean seawater. The acid was standardized by titrating weighed amounts of Na_2CO_3 dissolved in 0.7 M NaCl solutions. The acid factor was also determined by coulometry with an agreement of ±0.0001 M. The precision is better than 0.4 μmol kg^{-1}. The performance has been checked by titrating different batches of CRMs (nos. 32, 34, 35). An adjustment of the

acid factor from 0.2504 to 0.2505 M gave a better agreement with the certified values and was used in the computation of A_T.

3. Results and discussion

3.1. Distribution of nutrients and water masses

A composite section, instead of three separate sections, here is used to resume the thermohaline and chemical distribution in the three sampled transects (Fig. 2). The African coast therefore is at both ends of the plot, and the 18°W section is then situated at about the centre. The depth axis was modified using three different scales (0–1000, 1000–2000 and 2000–bottom). in order to better resolve the upper 2000 m. The upper salinity minimum centred at about 750 m depth is the lower end of the ENACW, which is characterised by a steady and strong gradient in salinity and temperature in the main thermocline. The isohaline of 35.66 defines the limit that separates the saline ENACWt from the fresher ENACWp (Harvey, 1982; Pollard and Pu, 1985). This isohaline closely follows the 12°C isotherm. So the ENACWt layer extends from the bottom of the surface layer down to 500 m. Below it, down to the salinity minimum of ENACW, there is a relatively narrow layer of ENACWp. The minimum of salinity is lower than 35.4 in the south–east corner at 800 m depth between Lanzarote Island and the African shelf, tracing the northward advection of AAIW (Willenbrink, 1982) as a poleward undercurrent of the Canary Current, but this cannot be traced with salinity further north than 32°N. The salinity minimum at 32°N was higher than 35.55 except for Stn. 63. Just at this station, there is a salinity maximum of 36.383 at 1283 m, corresponding to the core of the Meddy "Jani." Outside this Meddy, the salinity maximum generally decreases towards south and west. The Meddy is also discerned by its temperature maximum at 1200 m within a rather steady vertical gradient. Below MW, a continuous decrease of salinity and temperature denotes the presence of LSW and NADW. In the northern section, the salinity and temperature are slightly higher than at the southern section, probably related to the influence of MW (Arhan and King, 1995).

To remove the saline effect over A_T and C_T, normalised A_T ($NA_T = A_T/S35$) and normalised C_T ($NC_T = C_T/S35$) are shown. A steeper vertical gradient of NA_T was observed below the main thermocline in all sections and slightly higher values were found in the southern section. The silicate distribution showed also a pattern similar to that of NA_T (correlation between both variables is $r^2 = 0.96$ with $n = 403$ and a NA_T/SiO_2 ratio of 1.88 ± 0.02). Furthermore, we can observe a minimum of silicate and NA_T at the salinity maximum of MW. Between Lanzarote Island and the African coast, the maximum of SiO_2 of 16.6 μmol kg^{-1} close to the bottom (1200 m) is associated opal redissolution. The maximum influence of AAIW is recorded at 800 m by the minimum of salinity and pH_{SWS}.

On the other hand, NC_T, NO_3 and AOU distributions, affected by the regeneration of organic matter, show similar patterns and present high correlation ($r^2 > 0.77$) among them (Fig. 2). NC_T distribution is also affected by redissolution of $CaCO_3$. Phosphate distribution (not shown) is very similar to that of nitrate, with a high correlation between them ($r^2 = 0.98$, N:P $= 15.4 \pm 0.1$, $n = 472$). The domain of ENACW is characterised by a gradient of NC_T, NO_3 and AOU with values increasing from surface down to 800 m. The degree of ventilation of this water mass as deducted from the AOU distribution does not show significant differences in the upper thermocline. At deeper levels, the signal of the Meddy is clearly discerned by its moderate AOU values, a product of its low oxygen content and its warm temperature. However, the low nitrate levels and high pH_{SWS} of the Meddy suggest a relative low age. In the southeast, the influence of AAIW is manifested by its low AOU and pH_{SWS} values (149 μmol kg^{-1} and 7.636, respectively), and by an absolute nitrate maximum of 27 μmol kg^{-1} at Stn. 35, at 799 m depth. Below the layer of MW core and the poleward intrusion of AAIW, there is a relatively homogenous layer of nutrients, pH_{SWS} and AOU in relation to the layer immediately above. Below, the influence of LSW was only apparent in the northwestern part of the box by the AOU minimum (AOU < 80 μmol kg^{-1}) around 1800 m. Finally, deep waters presented high nutrient values (> 21

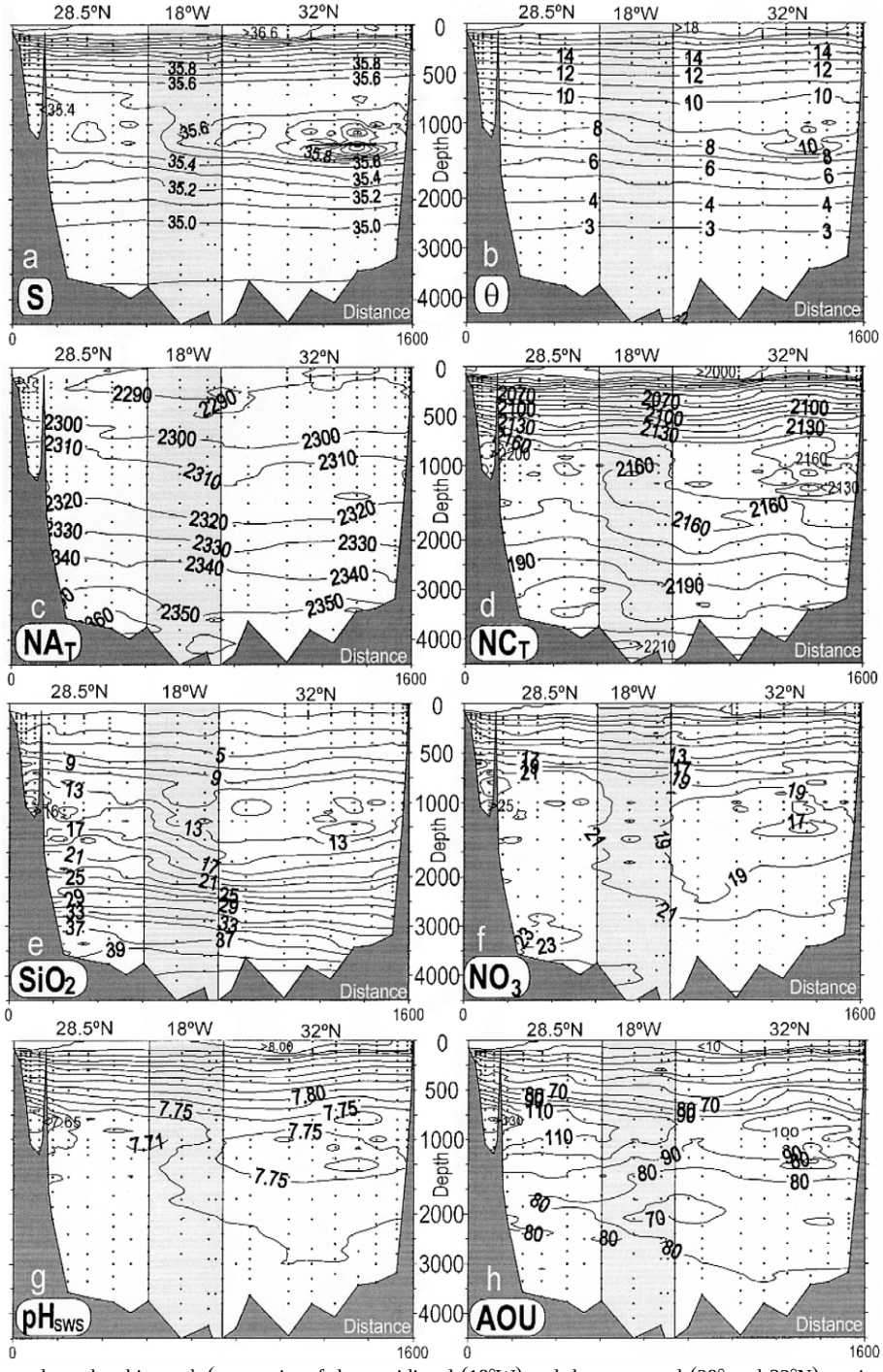

Fig. 2. Distributions along the ship-track (composite of the meridional (18°W) and the two zonal (29° and 32°N) sections) of salinity (a), potential temperature (b), normalised total alkalinity (c), normalised total inorganic carbon (d), silicate (e), nitrate (f), pH_{SWS} (g), and AOU (h). The units are in micromoles per kilogram except for salinity and pH. Stns. 49 and 55 are located at the corners on the 18°W meridian section (Fig. 1). Shaded area corresponds to the 18°W meridional section.

μmol kg^{-1}) and consequently, low AOU and pH_{SWS} being more pronounced in the southern section than in the northern one.

3.2. Mixing model

Following the water masses description given above, we define a set of end-members in order to describe the thermohaline variability due to mixing. It is not necessary to assume either isopycnal or diapycnal mixing. Fig. 3 shows a θ–S diagram with the whole set of samples. The high correlation between θ and S below 2.50°C yielded a linear relationship for NADW of $\theta = 11.1_{\pm 0.2} S - 385.0_{\pm 0.2}$ with $r^2 = 0.987$, which is similar to earlier observations (Saunders, 1986; Castro et al., 1998; Paillet et al., 1998). So we chose the lowest θ–S pair for the lower end-member of NADW (NADWl). For the upper limit of NADW (NADWu), we have used the same θ–S point as suggested by Castro et al. (1998) based on the lower limit of MW influence (Harvey, 1982). This θ–S point is very similar to the end-member used by Stoll et al. (1996) to define the Lower Deep Water in the Iceland basin. Regarding the LSW end-member, we have adopted the θ–S properties reported by Talley and McCartney (1982) when the LSW crossed the Mid Atlantic Ridge (3.40°C and 34.89). We have selected the thermohaline characteristics of MW (11.74°C and 36.5) from Wüst and Defant (1936) near Cape St. Vicente (Rhein and Hinrichsen, 1993). Finally, taking into account that ENACW is composed of two different sets of mode waters, the typical line defining ENACW (Sverdrup et al., 1942) has been divided into two segments corresponding to these two varieties; subtropical (ENACWt) and subpolar (ENACWp) mode waters (Harvey, 1982; McCartney and Talley, 1982; Ríos et al., 1992). We keep the same acronyms for the shallow and deep end-members of ENACWt and ENACWp, respectively. The area studied during the Meteor 37/2 cruise is close to the region of formation of the Madeira Mode Water (Siedler et al., 1987). According to these authors, this water mass

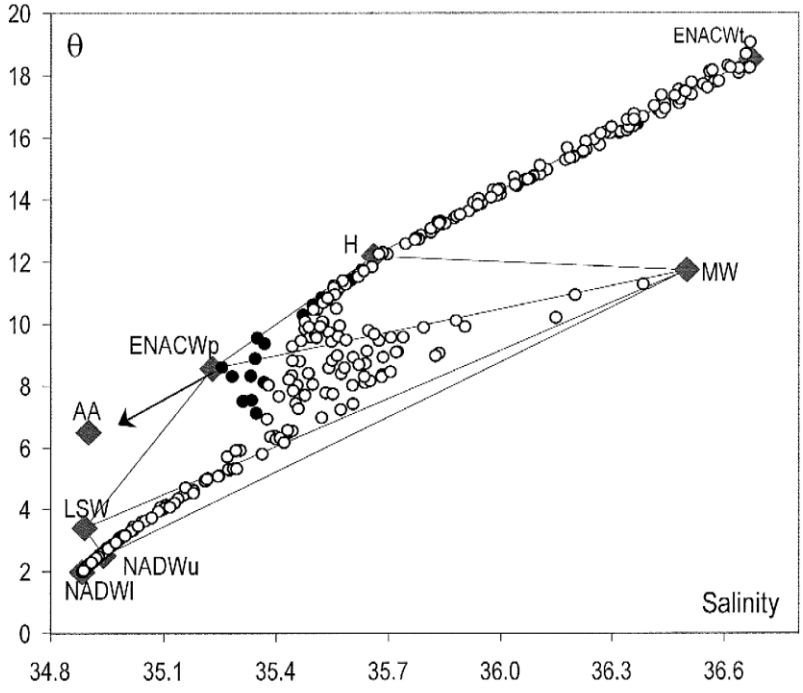

Fig. 3. θ–S diagram of the samples (surface samples excluded) of the MET37/2 cruise with the applied mixing triangles indicated. The black solid symbols represents the samples resolved using the AA end-member. The thermohaline properties of the water types are shown in Table 1.

corresponds to the mode water with the highest volumetric census in the Eastern Subtropical Atlantic, and consequently we have considered their θ–S properties for the ENACWt end-member (18.5°C, 36.675). On the other hand, we have chosen 12.2°C and 35.66 as the lower limit of ENACWt and, consequently, the upper limit of ENACWp following Harvey (1982). Thus, the latter θ–S pair, represented by H (Fig. 3), has been selected to separate ENACWt from ENACWp. Following the earlier paper of Castro et al. (1998), the ENACWp end-member has a temperature of 8.56°C and salinity of 35.23, establishing the triangle of mixing between ENACWp (H-ENACWp) and MW without LSW contribution (Fig. 3), since the contribution of LSW occurs below the salinity maximum of MW (below 1100 m depth). The mixing below the core of MW is quantified from the triangle ENACWp, MW and LSW. Thus, the ENACWp-MW line joins the MW maximum in each profile.

Between the Lanzarote island and the African coast (Stns. 27–35), the AAIW influence is evident for salinities lower than 35.4 (Fig. 2a) as commented before. In order to evaluate the influence of AAIW in this channel, the ENACWp point is replaced by the AA end-member (Fig. 3), whose thermohaline characteristics (6.5°C and 34.9) have been defined by Fraga et al. (1985) off Cape Blanc ($\sim$ 20°N) and are similar to those measured by Tsuchiya et al. (1992) at 20°N and 20°W. The term AAIW must only be used for the water mass of 4°C and salinity of 34.2 formed in the Subantarctic front at about 45°S (Reid, 1994).

Taking into account that the distributions of thermohaline and chemical parameters are strongly influenced by the spreading of MW and the influence of AAIW in the studied area, we employ this triangular mixing approach to estimate the contribution from each source. The triangles are established in a way that one side of the triangle corresponds to a layer of mixing between maximum and minimum of salinity and, consequently, samples above this layer do not mix with samples below it and belong to another triangle. The samples from sea surface to the first upper salinity maximum, about 100 m, are excluded from the analysis because their thermohaline properties are altered by atmospheric conditions and do not follow a conservative behaviour. The ENACWp and NADW water mass was modelled by the segments H-ENACWt and NADWl-NADWu, respectively.

The contribution of the water masses considered ($M_{k,i}$) to a given sample i can be calculated solving the following determined system of three linear equations:

$$1 = \sum M_{k,i}$$
$$S_i = \sum M_{k,i} S_k$$
$$\theta_i = \sum M_{k,i} \theta_k, \quad (1)$$

where k is the water mass (ENACWt, H, ENACWp, MW, AA, LSW, NADWu, NADWl) and i is the sample number (from 1 to 408). S_k and θ_k are the thermohaline characteristics of the k water mass end-member. As each sample is comprised within the limits of an unique triangle or θ/S segment, $M_{k,i}$ must be set to zero for the other four water masses. Once $M_{k,i}$ had been calculated for the 408 samples, the expected concentration of any chemical variable for the six end-members in the study area (C_k) was obtained by solving the corresponding 408 equations by a least squares approach (Castro et al., 1998; Pérez et al., 1998):

$$C_i = \sum M_{k,i} C_k. \quad (2)$$

As any multilinear fitting, this procedure also provides the theoretical values of the variable C_k and the residual or anomaly for every sample.

3.3. Validation by conservative tracers

In order to support the proposed mixing model, we have applied the equation system (2) to two conservative tracers. Following Broecker (1974), we have used the tracer 'NO' with an R_N of 9.33 (Anderson, 1995; Fraga et al., 1998) to eliminate the effect of remineralization of organic matter (ROM) on the nitrate and oxygen variability. The mixing model explains 98.6% of 'NO' variability (Table 1). The standard deviation of 'NO' residuals (9 μmol kg^{-1}) is half of the one expected from the combination of the residuals of nitrate and oxygen ($1.2 \cdot 9.33 + 7.2 = 18.4$ μmol kg^{-1}). Ríos et al. (1998) introduced a new combined chemical tracer 'NCO,' which improves the conservative behaviour of 'NO.' In nutrient-depleted waters or in damaged phytoplankton cells, the synthesis of organic matter does not

Table 1
The definition of the eight water types and their chemical characterisation obtained from the mixing model using 408 water samples

	S	θ	O_2	AOU	NO_3	SiO_2	PO_4H_2	C_T	A_T	pH_{SWS}	'NO'	'NCO'
ENACWt	36.675	18.50	229 ± 1	-1	0.4 ± 0.2	0.3 ± 0.2	0.01 ± 0.01	2090 ± 1	2397 ± 0.5	8.004 ± 0.002	233 ± 2	2320 ± 1
H	35.660	12.20	194 ± 1	67	13.7 ± 0.2	4.9 ± 0.2	0.79 ± 0.01	2148 ± 1	2336 ± 0.5	7.808 ± 0.002	322 ± 2	2379 ± 1
ENACWp	35.230	8.56	157 ± 2	125	24.5 ± 0.3	14.5 ± 0.4	1.55 ± 0.02	2189 ± 2	2321 ± 1.0	7.685 ± 0.003	386 ± 3	2412 ± 2
AA	34.900	6.50	119 ± 4	177	29.7 ± 0.6	19.9 ± 0.7	1.92 ± 0.04	2218 ± 3	2312 ± 1.7	7.582 ± 0.005	396 ± 4	2417 ± 3
MW	36.500	11.74	192 ± 4	68	11.9 ± 0.6	7.2 ± 0.7	0.67 ± 0.04	2205 ± 3	2414 ± 1.7	7.831 ± 0.005	304 ± 4	2430 ± 3
LSW	34.890	3.40	237 ± 2	80	22.5 ± 0.4	19.5 ± 0.4	1.46 ± 0.03	2172 ± 2	2316 ± 1.1	7.704 ± 0.005	446 ± 3	2470 ± 2
NADWu	34.940	2.50	248 ± 1	79	21.4 ± 0.2	34.8 ± 0.3	1.40 ± 0.02	2191 ± 1	2344 ± 0.7	7.728 ± 0.002	447 ± 2	2497 ± 1
NADWl	34.884	1.98	245 ± 2	86	23.2 ± 0.3	44.4 ± 0.3	1.50 ± 0.02	2204 ± 2	2353 ± 0.8	7.722 ± 0.002	462 ± 2	2513 ± 1
r^2			0.93		0.97	0.986	0.970	0.967	0.967	0.989	0.987	0.992
SD			7.2		1.2	1.4	0.086	6.7	3.3	0.010	8.3	5.6

always follow the stoichiometric ratio of average phytoplankton composition due to the synthesis of an excess of carbohydrates (Cullen et al., 1985; Villarreal et al., 1999). Ríos et al. (1998) combined the synthesis of carbohydrates and the typical composition of phytoplankton to define:

$$\mathrm{NCO} = \mathrm{O_2} + \mathrm{CO_2} + \mathrm{NO_3} R_\mathrm{N}(1 - 1/R_\mathrm{C}) = \mathrm{NO} + (\mathrm{CO_2} - \mathrm{NO_3} R_\mathrm{N}/R_\mathrm{C}).$$

The second summand of the last term accounts for the synthesis or mineralization of the carbohydrate excess over the typical organic matter synthesis of phytoplankton (Fraga and Pérez, 1990; Laws, 1991; Ríos et al., 1998). R_N of 9.33 and R_C of 1.41 are the stoichiometric ratios of this average synthesis. The mixing model explains 99.1% of 'NCO' variability, which is higher than that of 'NO' (Table 1 and Fig. 4a). The standard deviation of 'NCO' residuals (5.6 μmol kg^{-1}) is three times lower than the one expected from the combination of the residuals of 'NO', nitrate and CO_2 (Table 1). The distribution of 'NCO' residuals (Fig. 4b) is very patchy and does not present clear relation with the distribution of 'NCO' or any other biogeochemical variable. So, the high variability of 'NO' and 'NCO' predicted by the mixing model supports the quality of the model.

In contrary to 'NO' or 'NCO,' nitrate, oxygen and C_T in subsurface waters are affected by ROM. Therefore, they do not completely behave as conservative variables. However, we shall apply the model to these variables, assuming a conservative behaviour (Pérez et al., 1993, 1998; Castro et al., 1998). We should expect a less percentage of explained variance for these chemical properties due to ROM. The AOU distributions clearly showed the patterns of the ROM accumulate in the water masses since its formation (Redfield et al., 1963; Broecker, 1974). The vertical profiles of AOU (Fig. 2h) along the studied region are quite similar and the model fits a great part of AOU variability. So, part of the C_T, A_T, nitrate and silicate variability caused by ROM is also included in the values of the end-members. The mixing model splits their variability in two parts, one is included in the nutrient concentrations predicted by the model-derived end-members and the other part is included in the residuals and mainly related to the ROM in the studied area. This partition depends on the average residence time of the water masses in the study area. As the residuals vary independently from θ and S, their distributions can be related with the variability of the ROM within the area; this will be commented on in Section 3.4.

3.4. Output of mixing model: chemical characterisation of the water masses

In Table 1, we show the nutrient end-members obtained after applying the mixing model. The variances explained by the application of the model for the distribution of C_T, A_T, nitrate and silicate are greater than 96.7%, while the variance explained for oxygen is slightly lower (93%). This difference in the proportion of not-explained variability is related to the magnitude of the total natural variance of each chemical tracer. The range of variation in the oxygen end-members is lower than the one of nitrate, if the stoichiometric ratios ($\Delta\mathrm{P}{:}\Delta\mathrm{N}{:}\Delta\mathrm{C}{:}\Delta\mathrm{O_2} \equiv 1{:}16{:}106{:}149$) of ROM are taken into account (Anderson, 1995; Fraga et al., 1998). The ratios of variance not explained by the model are $\Delta\mathrm{P}{:}\Delta\mathrm{N}{:}\Delta\mathrm{C}{:}\Delta\mathrm{O_2} \equiv 1{:}14{:}79{:}83$ (Table 1), being of the same order than the stoichiometric ratios. In addition, the combined variables 'NO' and 'NCO' defined in order to remove the effects of ROM are much better fitted than O_2 and nutrients. Silicate is less affected by redissolution than the other nutrients and presents a slightly better fit. The model defines very well the A_T end-members and its natural variability. Errors of both A_T end-members and residuals are close to the analytical errors.

The nutrient end-members summarise the chemical variability of the water masses. The AOU end-members show low values (young waters) only in the upper ocean. The subtropical region is far from the outcropping region of most water masses involved in the sampled area. Deep waters, including LSW, show similar AOU values and rather similar nutrients concentrations and $\mathrm{pH_{SWS}}$. The AA end-member is the oldest, probably due the influence of AAIW, which takes a long time to travel from its formation area and passes upwelling areas with strong biological activity. Although its nitrate, phosphate and AOU levels are very high, its silicate content is not as high compared to the one observed in the

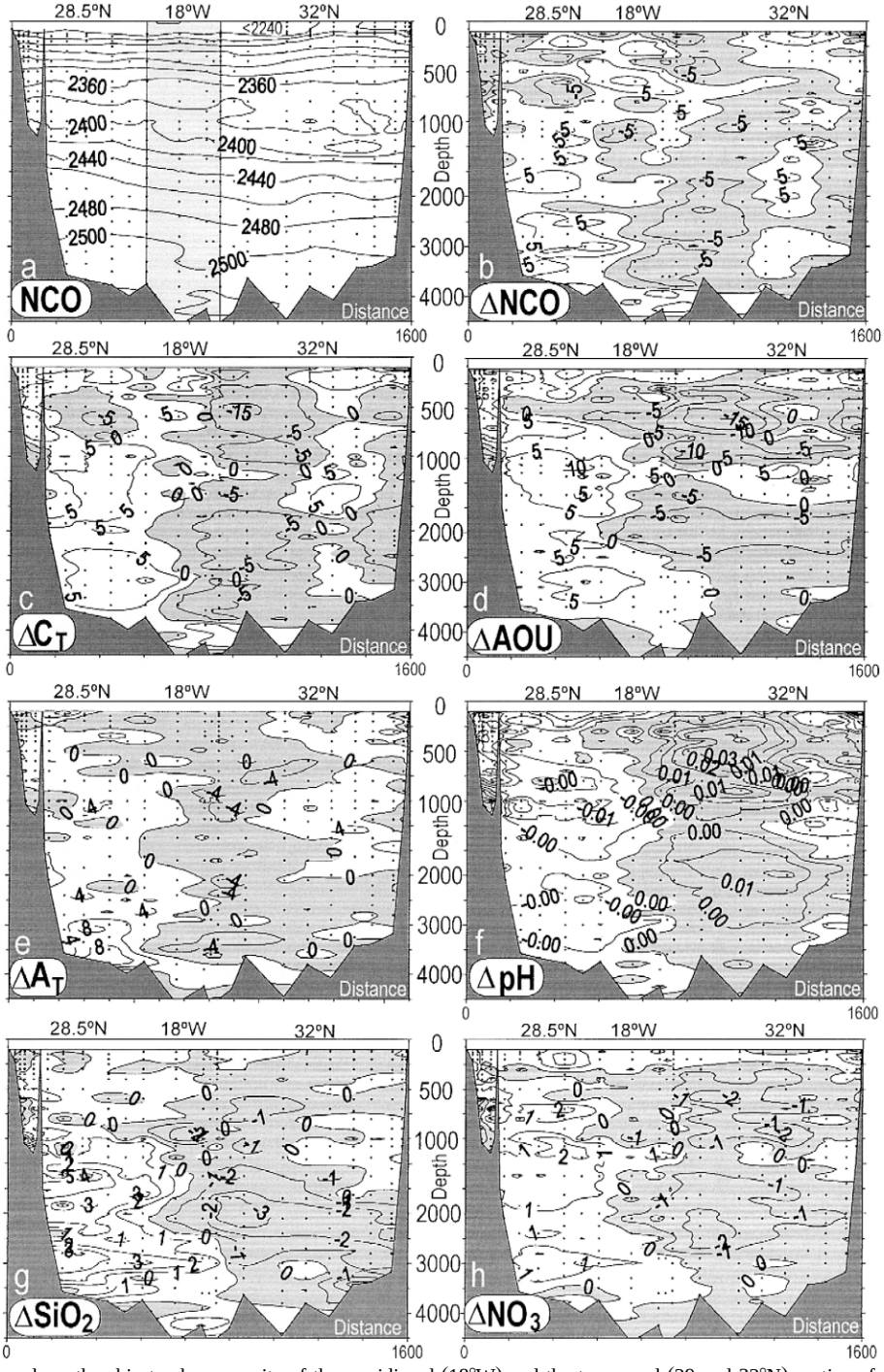

Fig. 4. Distribution along the ship-track composite of the meridional (18°W) and the two zonal (29 and 32°N) sections for 'NCO' (a), and anomalies of 'NCO' (b), C_T (c), AOU (d), A_T(e), pH_{SWS} (f), silicate (g) and nitrate (h). Except for pH, all units are in micromoles per kilogram.

equatorial region (about 30–35 μmol kg^{-1}). When the AAIW crosses the North Equatorial Current, it suffers a strong dilution with the waters present north of the subtropical gyre, mainly, ENACW and MW. With similar temperature, the upper limit of the subpolar ENACW (H) and the MW present similar levels of AOU, pH_{SWS} and nutrients, though they are probably younger than the AA and ENACWp end-members. The extrapolation from the H-ENACWp segment to AA using temperature as master variable yields to higher oxygen concentrations in a 13% and a slightly higher nitrate than those values given by the mixing model.

3.5. Remineralization of organic matter and distributions of residuals

The distribution of residuals (measured minus modelled values) shows a defined, non-randomised behaviour and a similarity among C_T, oxygen, pH_{SWS} and nutrients (Fig. 4). Once the variability caused by mixing is removed with the mixing model, the residual variability can be mainly ascribed to either ROM or dissolution of hard parts of biogenic matter. ROM affects mainly oxygen, pH_{SWS}, nitrate and C_T, and redissolution increases silicate, C_T and A_T. White areas in Fig. 4c–h indicate regions where both processes increase the levels of nitrate, silicate, AOU, NC_T, NA_T and decrease pH_{SWS}, while shaded areas are related to recent advection of seawater (relatively new) into the area. The spatial distribution of white and shaded areas is rather coincident in the whole set of residual maps. Phosphate anomalies (not shown) present a rather similar pattern. The correlation between phosphate and nitrate residuals is $r^2 = 0.49$ with a N:P ratio of 13.8 ± 0.7. The AOU and nitrate residuals also show a significant correlation ($r^2 = 0.41$) with R_N of 6.1 ± 0.3, which is somewhat lower than expected from ROM. The AOU and C_T residuals present a better correlation ($r^2 = 0.48$), with R_C of 1.1 ± 0.06, which is also lower than expected by ROM (Takahashi et al., 1985; Minster and Boulahdid, 1987; Anderson, 1995; Ríos et al., 1998). The small extension of the study area and the good fit of the model yield low variances of the residuals and therefore, no high correlation between them should be expected. The analytical error is also included in the residual distribution, thus reducing the correlation and estimated ratios. The best correlation between residuals was obtained between pH_{SWS} and AOU ($r^2 = 0.66$) with a ratio $\Delta AOU{:}\Delta pH_{SWS}$ of 729 ± 26. If the oxygen data are included to calculate the pH_{SWS} values, the correlation between real and modelled data rises from $r^2 = 0.989$ to 0.995, decreasing the standard deviation of residuals from 0.0099 to 0.0061, slightly higher than the expected analytical error (0.004).

Spencer (1975) reported ratios of $\Delta Si/\Delta N$ between 0.5 and 1.2, which implies a ratio R_{Si} ($= -\Delta O_2/\Delta Si$) from 9 to 20. We found here low and significant covariation between silicate and oxygen residuals ($r^2 = 0.14$, $n = 403$) with R_{Si} of 10 ± 3, similar to the one calculate previously in the Eastern North Atlantic (Pérez et al., 1993, 1998; Castro et al., 1998). However, in deep waters (depth > 1500), the correlation is higher ($r^2 = 0.49$, $n = 150$) with R_{Si} of 2.7 ± 0.1, in agreement with that estimated by Castro et al. (1998) in deep waters between 39° and 48°N.

The similarity between the ratios calculated here and those reported in the literature supports the idea that the residuals of the mixing model are mainly due to ROM or redissolution of hard structures, which are strongly dependent on the residence time of the water masses in the area. Taking into account that the geographical distributions of the anomalies (Fig. 4) of the different variables show a very similar behaviour, the results of nutrients and oxygen anomaly can be described in terms of aging or ventilation. Generally, the northern section shows clearly lower nutrients, C_T, A_T and AOU (higher pH_{SWS}) than the southern one with the 18°W meridional section as a transition between the two zonal sections. The north–north–east to south–south–west advection of water masses in practically all levels (Reid, 1994; Paillet and Mercier, 1997) introduces relatively younger water from the north and the effect of the high productivity upwelling area close to the African coast could contribute to the increase of nutrients in the southern section. The poleward intrusion of waters with AAIW characteristics between the Lanzarote island and the African coast (Stns. 33 and 35) creates a maximum of ROM (negative pH_{SWS} and positive C_T, AOU and nitrate anomalies) between 500 m and the salinity minimum at 800 m depth. Below, there exists a bottom layer

with relatively low ROM. Also, the deep Meddy seems to introduce a mesoscale structure in the ROM pattern.

3.6. Comparison with data outside the study area

A similar mixing analysis has been made in other areas of the Eastern North Atlantic Basin. Pérez et al. (1993) used data from several cruises between 40° and 47°N and 8° and 11°W and provided the chemical characterisation of the water masses close to the Iberian Peninsula from 100 to 2500 m depth and made a comparison with data from other areas of the North Atlantic using chemical conservative tracers. Castro et al. (1998) used data from the Vivaldi cruise (39–48°N and 9–24°W) to resolve the chemical characterisation of the same water masses as in the present study and validate their results using the data from Transient Tracer Ocean (TTO). Data from two sections along 22°W and 41°N resulting from the ANA cruise (Ríos et al., 1992) allowed to fit the chemical variability of the water masses in the upper 1100 m (Pérez et al., 1998) including the influence of AAIW and resulted in a good comparability with data from TTO and from the area of the Mauritania upwelling (TTO, 1981; Manríquez and Fraga, 1978). Taking into account data from several cruises in the European Basin from 31° to 53°N, van Aken (2000b) has recently made the chemical characterisation of water masses using isopycnal analysis. The chemical characterisation from the latter work is included in the Table 2, together with the results obtained here.

3.6.1. Central waters

The ENACW is composed from several source water (subtropical and subpolar) and is affected by the northward spreading of AAIW. In addition, the salinity maximum of ENACW varies latitudinally, thus introducing different ENACWt end-members. To study the agreement between different data bases, Fig. 5 shows the main covariation between conservative and non-conservative variables. The spatial variability in the ventilation of ENACW results in different values for the non-conservative chemical tracer for a given end-member. However, this behaviour is constrained by the ratios of variability of the ROM. The nitrate and phosphate values of ENACW end-members present a very high correlation ($r^2 = 0.995$, $NO_3 = 15.15PO_4 + 1.25$). Also the C_T/A_T ratio ($=$ Xca), which has a very strong relation with pH_{SWS}, shows a high linear correlation (Fig. 5a). Although the recycling of silicate and nitrate follows different pathways, the values of the end-members show a very high non-linear correlation, which reveals increase of SiO_2:NO_3 ratio with depth due to the increase of redissolution of opal skeletons and decrease of ROM. Also, the AOU and nitrate end-member values showed high correlation ($r^2 = 0.94$), resulting in a very linear behaviour of the conservative tracer 'NO' (Fig. 5b) and 'PO.'

A simple and conservative chemical variable, C_T^*, could be defined from C_T in similar way as preformed nitrate (Broecker, 1974) if the C_T values are corrected for ROM using AOU and $R_C = 1.41$:

$$C_T^* = NC_T - AOU/R_C.$$

The C_T^* values for the end-members of ENACW show a very good correlation with θ and are also in agreement for the different data bases. However, the C_T value for the AA end-member observed during the ANA cruise gave lower values for Xca and C_T^* compared to those observed here. The ANA cruise went south of 20°N, where the influence of AAIW is higher. Given the anthropogenic influence on C_T, Xca and C_T^*, the C_T of AA is lower by about 10–20 μmol kg^{-1} compared to ENACW (Pérez et al., 1998).

3.6.2. How is the actual advection of AAIW along the eastern boundary?

Assuming a conservative behaviour of silicate, Tsuchiya (1989) extended the intrusion of AAIW beyond 45°N. The physical and chemical characteristics of the AAIW end-member used by van Aken (2000b) are very similar to those of the ENACWp end-member proposed in this work and previous works for the European basin (Willenbrink, 1982; Harvey, 1982; McCartney and Talley, 1982; Arhan et al., 1994; Castro et al., 1998). van Aken (2000b) considered that the salinity minimum of ENACWp indicates the presence of AAIW. However, several authors (Harvey, 1982; McCartney and Talley, 1982; Arhan et al., 1994) described the formation of subpolar mode water in the European Basin with salinities from 35.40 to 35.66 and its southward spreading from 43° to 48°N to the Subtropical gyre. Käse et al.

Table 2
Calculated chemical properties of the water masses of Eastern North Atlantic from several papers
ANA, IBERIA, VIVALDI, van Aken and ICELAND refer to the papers: Pérez et al. (1998), Pérez et al. (1993), Castro et al. (1998) and van Aken (2000a,b) and Stoll et al. (1996), respectively.

Reference	S	θ	γ_{500}	'NO'	'PO'	C_T^*	O_2	AOU	NO_3	PO_4	C_T	A_T	SiO_2	Type
ENACW														
MET37/2	36.672	18.50	28.607	233	231	1994	229	0	0.4	0.01	2090	2397	0.3	ENACWt
IBERIA	35.815	13.71	29.094	285	279	2045	233	20	5.6	0.32	2107	2347	1.6	ENACWt
ANA	36.500	18.00	29.604	229		1989	195	37	3.6		2100	2380	2.0	ENACWt
VIVALDI	36.120	14.86	29.073	277	264	2022	228	19	5.2	0.25	2100	2355	2.0	ENACWt
MET37/2	35.660	12.20	29.292	322	307	2061	194	67	13.7	0.79	2148	2336	4.8	H
ANA	35.660	12.00	29.333	317		2057	213	49	11.2		2131	2338	4.5	H
VIVALDI	35.660	12.20	29.292	331	316	2069	254	7	8.2	0.43	2113	2336	2.8	H
MET37/2.	35.230	8.56	29.633	386	380	2085	157	126	24.5	1.55	2189	2321	14.6	ENACWp
IBERIA	35.300	9.40	29.544	371	360	2084	200	78	18.3	1.11	2157	2325	8.1	ENACWp
ANA	35.230	8.58	29.629	378		2090	185	98	20.7		2174	2323	11.9	ENACWp
VIVALDI	35.230	8.56	29.633	373	356	2091	199	84	18.7	1.09	2165	2315	9.7	ENACWp
MET37/2	34.900	6.50	29.696	396	396	2097	119	178	29.7	1.92	2218	2312	19.9	AA
ANA	34.900	6.50	29.696	429		2088	116	181	33.6		2211	2306	24.1	AA
van Aken, 2000b	35.420	9.43	29.632	360	357		170	107	20.4	1.3			11.5	AA

Reference	S	θ	γ_{2000}	'NO'	'PO'	C_T^*	O_2	AOU	NO_3	PO_4	C_T	A_T	SiO_2
MW													
MET37/2	36.500	11.74	31.589	304	289	2067	193	69	11.9	0.67	2205	2414	7.2
IBERIA	36.500	11.74	31.589	307	294	2053	166	96	15.1	0.89	2209	2417	10.4
ANA	36.500	11.76	31.584	308		2053	163	99	15.5		2212	2413	10.6
VIVALDI	36.500	11.74	31.589	305	295	2054	145	117	17.1	1.04	2225	2409	11.3
van Aken, 2000b	36.500	12.01	31.527	305	291		177	83	13.7	0.79			7.6
LSW													
MET37/2	34.890	3.400	31.907	447	448	2120	237	83	22.5	1.47	2172	2316	19.5
IBERIA	34.890	3.400	31.907	434	441	2122	261	59	18.5	1.25	2157	2307	14.7
VIVALDI	34.890	3.400	31.907	435	423	2125	270	50	17.7	1.06	2154	2295	10.9
ICELAND	34.890	3.400	31.907	436		2116	280	40	16.7		2141		10.5
van Aken, 2000a	34.890	3.428	31.903	437	440		279	40	16.9	1.12			10.3
NADW— upper													
MET37/2	34.940	2.500	32.073	448	450	2138	248	79	21.4	1.40	2191	2344	34.8
IBERIA	34.925	2.400	32.075	445	450	2136	248	80	21.1	1.40	2188	2337	37.4
VIVALDI	34.940	2.500	32.073	439	438	2131	253	74	19.9	1.28	2180	2326	30.4
ICELAND	34.940	2.500	32.073	436		2134	249	82	20.4		2183	2326	35.3
van Aken, 2000a	34.936	2.500	32.070	440	447		249	71	20.5	1.38			33.6
NADW— lower													
MET37/2	34.884	1.980	32.099	462	462	2150	245	86	23.2	1.51	2204	2353	44.4
VIVALDI	34.890	2.030	32.097	452	469	2152	238	93	22.9	1.60	2211	2354	46.9
van Aken, 2000a	34.889	1.984	32.102	452	462		245	86	22.2	1.50			46.3

(1986) described the spreading of this subpolar mode water throughout the Canary basin. Paillet and Mercier (1997) traced the southward spreading of $ENACW_P$ from 44° to 25°N by a minimum in potential vorticity. In the upwelling area, from the depth of ENACW to the bottom, Reid (1994) described a maximum of AOU at 24°N and its northward spreading making up a steep north–south gradient of AOU and nutrients north of the Canary Islands, similar to the one described here. The most striking feature

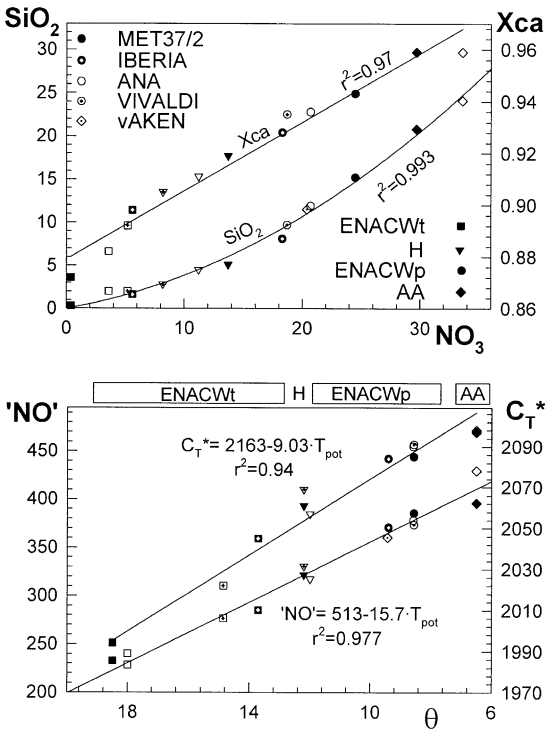

Fig. 5. Chemical characterisation of ENACW (ENACWt: squares; H: triangles; ENACWp: circles; AA: diamond) from different authors and data sets (MET37/2: black; IBERIA: cross inside black symbol; ANA: open symbol; VIVALDI: symbol inside open circle; van Aken, 2000b: little cross inside diamond). Upper panel: Covariation between silicate and Xca(C_T / A_T) vs. nitrate. Lower panel: Variation between conservative tracers 'NO' and C_T^* vs. potential temperature. The curve fits the silicate vs. nitrate in second order. Except for Xca and θ, all units are in micromoles per kilogram.

showed by Reid (1994) at $\gamma_{1000} = 32$ is a strong silicate increase along the NW coast of Africa, suggesting the strong effect of the productive upwelling water on the biogeochemical behaviour of deep waters. Enhanced productivity and consequently ROM in the coastal upwelling off North Africa both play a significant part in creating the tropical oxygen minimum in the eastern North Atlantic (Kawase and Sarmiento, 1986). The oxygen minimum must be also physically isolated from direct ventilation with the atmosphere (Doney and Bullister, 1992). So, these combined biogeochemical processes and its north–south gradient could tend to an incorrect description of the presence of AAIW at latitudes north of 24°N, if it is traced on basis on nutrient maxima.

The use of conservative chemical tracers can give information about the real water masses contribution in the layer between 500 and 1000 m. The 'NO' and C_T^* values of AAIW ($\theta = 3.9$°C, $S = 34.2$) in its formation area at the SAF (Sub Antarctic Front) are 518 and 2165 μmol kg^{-1} (Le Groupe CITHER-3, 1998). When reaching 10°S, AAIW has partially mixed with South Atlantic Central Water and NADWu, thus increasing salinity and temperature (34.5 and 4.67°C) and decreasing 'NO' and C_T^* values (472 and 2135 μmol kg^{-1}). At this latitude, the nutrients reach maximum values (Reid, 1994) due to ROM. Nitrate and silicate concentrations rise to 35.6 and 32.9 μmol kg^{-1}, respectively (Le Groupe CITHER-3 , 1998). At 10°N, the minimum of salinity, which is a typical indicator for the spreading of AAIW, is higher than 34.9, and its 'NO' and C_T^* values decrease to 459 and 2095 μmol kg^{-1}, respectively. Data from the ATLOR cruise, at 20°N close to the African coast, yielded 'NO' values of 420 μmol kg^{-1} for AAIW with 6.5°C (Manríquez and Fraga, 1978). The chemical characterisation of the end-member AA by using data from ANA cruise (24–28°N and 22°W) yielded similar results for 'NO' (429 μmol kg^{-1}) and C_T^* (2088 μmol kg^{-1}). The presence of AAIW decreases from 100% in the SAF to 75% at 10°S, to 64% at 10°N and to 45% at 24°N, if linear mixing is assumed with a northern component of thermohaline (9.4°C and salinity of 35.3) and chemical (371 and 2089 μmol kg^{-1} for 'NO' and C_T^*, respectively) characteristics similar to the subpolar mode water described by Pérez et al. (1993) and van Aken (2000b) north of 40°N. The 'NO' of the AA end-member is 396 μmol kg^{-1} with 17% of pure AAIW and 83% of ENACWp end-member. During the MET37/2 cruise, the sample (Stn. 35, 800 m) with the salinity minimum caused by the influence of AAIW was about 35.3 (resolved by the mixing model as 69% of AA and 29% of MW). So the maximum percentage of pure AAIW was about 11% in the poleward undercurrent between Lanzarote Island and the African Coast. From thermohaline data, several authors had previously reported (Willenbrink, 1982; Käse et al., 1986; Reid, 1994) that AAIW is quickly diluted with ENACWp north of 20°N. So, the increase of nutrients and AOU along the African Coast is due to the remineralization processes linked to the upwelling system

(Kawase and Sarmiento, 1986; Reid, 1994; Doney and Bullister, 1992). In addition, the chemical characterisation proposed by van Aken (2000b) for AAIW corresponds closely to the one for ENACWp associated with a salinity minimum located above the MW in the European Basin. (Pérez et al., 1993, 1998; Castro et al., 1998). In the Canary Basin at 34°N, Käse et al. (1986) also ascribed the salinity minimum and O_2 maximum above MW to ENACWp.

Östlund and Rooth (1990) noted a decrease with time of the northward spreading of AAIW between 20° and 30°N and the southward penetration of LSW between 40° and 30°N when they compared the radiocarbon distribution from GEOSECS and TTO data. Recently, Lavin et al. (1998) have calculated the meridional transport and heat flux using three sets of hydrographic data from October 1957, August 1981 and July 1992 along 24.5°N. Their results show a progressive decrease of northward transport of AAIW from 1957 to 1992. The transport of water with temperatures between 6° and 9°C was 3.2 Sv in 1957, 2.1 Sv in 1981 and only 0.6 Sv in 1992, even showing a reversed evolution of transport at the 7°C level. These authors showed also a parallel decrease of southward transport of LSW along 24.5°N. All these independent calculations and measurements agree towards a progressive decrease of the northward spreading AAIW during the last decades and may explain the contradiction in the physical and chemical characterisation of AAIW as observed by Tshuchia (1989) using GEOSECS data, and the other recent descriptions (Willenbrink, 1982; Käse et al., 1986; Pérez et al., 1993, 1998; Castro et al., 1998).

3.6.3. Deep waters

The agreement among cruises for the chemical characterisation of MW is fairly good, especially using conservative tracers as 'NO,' 'PO' and C_T^*. However, the C_T^* value obtained from MET37/2 is rather high, about 0.6%, relative to the other three cruises. A part of this difference could be due to the anthropogenic CO_2 input. AOU and nutrient values of the MW end-members suggest a higher ventilation of MW during the MET37/2 than during the IBERIA and ANA cruises. On the other hand, MW in the VIVALDI cruise showed lower ventilation with high AOU and nutrients compare to the other cruises. The biogeochemical relations are quite consistent. Silicate concentrations in the MW end-members show lower values when sampled near the Gibraltar Strait (van Aken, 2000b) and/or within a strong Meddy (MET37/2). The A_T values for MW are also coherent (2413 ± 3 μmol kg^{-1}).

At 25°N, Doney and Bullister (1992) had dated the age of a Meddy (about 12–20 years) during the Oceanus 202 cruise using CFC analysis. These authors also found that the CFC values are lower in the salinity maximum of MW and higher in the salinity minimum above it. From 5° to 20°N, Doney and Bullister (1992) reported CFC concentrations in the AAIW ($S < 35$) at or below the blank levels. So, the seawater above MW must have been recently ventilated and therefore is ENACWp and not AAIW.

For LSW, we found a similar coherence in the chemical characterisation with a ventilation pattern just opposite to the previous described for MW. The conservative tracers 'NO,' 'PO' and C_T^* show good agreement. Probably, the slightly high 'NO' value calculated for MET37/2 can be ascribed to a higher influence of Southern Atlantic waters. The AOU and nutrients are high in the MET37/2 area due to a lower ventilation of LSW in this region compared to more northern areas (VIVALDI and Iceland Basin). Only a small amount of LSW arrives at the African coast after a long way in a cyclonic eddy (33°–43°N) and also affected by lateral mixing with MW (Reid, 1994). At the depth level of LSW (1800 m), MW spreads southwards to the Canary Islands, generating a north–south gradient of AOU and nutrients. In the Canary Basin, Käse et al. (1986) described a MW tongue separating ENACWp and LSW (NW) from AAIW (SE).

The chemical characterisation of both NADW end-members is fairly good. 'NO,' 'PO' and C_T^* obtained from the MET37/2 and the IBERIA cruises are very similar; this is also true for AOU and nutrients. The characterisation derived from the VIVALDI data set is very similar to that given by van Aken (2000a) and Stoll et al. (1996) using data from a cruise in the Iceland Basin. However, between both pairs of data sets, there are small differences. The AOU and nutrients of the NADWu sampled in the MET37/2 cruise are higher than the levels reported for the area north of 42°N. Reid (1994) showed a pronounced change of nutrients between the Canary Islands and the Gibraltar Strait, related to the down-

ward intrusion of MW. This spatial variability in NADW practically disappears at the NADWl level. Its chemical characterisation is in agreement for all the variables and for all the cruises, except for the low (by 5%) silicate values measured during MET37/2. A deep silica tongue along 24°N, with a maximum close to the African coast, and a steep northward decreasing gradient introduce variability in the silicate distribution between the levels of the 2° and 3°C isotherms in the Canary Basin (Speer, 1993; Reid, 1994).

Normalised alkalinity shows a very close relation to silicate (Ríos et al., 1995). There is a good correlation between NA_T and silicate values for the end-members (shown in Table 2) gives a high correlation ($NA_T = 2289_{\pm 2} + 1.5_{\pm 0.1}SiO_2$, $r^2 = 0.91$, $n = 24$) with an average error of 6 μmol kg^{-1}. The similar time scale for the dissolution of hard biogenic structures (opal and $CaCO_3$) probably leads to this good correlation (Broecker and Peng, 1982).

4. Conclusions

Application of our simple mixing model for the water masses found in Subtropical Eastern North Atlantic in January 1997 can explain more than 93% of the chemical variability. The percentage of explained variance is higher for the chemical conservative parameters "NO," "NCO" and C_T^* as the effect of remineralization of organic matter is removed.

The geographical distributions of model residuals clearly discern a region of relatively more ventilated waters, associated with the core of the Azores Current.

From the comparison of the modeled nutrient distribution with data obtained from similar mixing analysis in other regions of the Eastern North Atlantic, we can conclude: (1) the limit of the northward advection of AAIW was localized at 28.5°N in the study region being strongly diluted (to $< 11\%$ of pure AAIW) by MW and by ENACWp; (2) MW seemed to be more ventilated in the Meteor 37/2 region probably related to the presence of a Meddy; (3) modeled nutrients in the core of LSW were higher than the modeled nutrients for regions further north, as expected if considering the southward advection of this water mass. Furthermore, the upwelling system off Northwest Africa is the main responsible factor for the southward increase of nutrients, AOU and NC_T.

Acknowledgements

The authors thank the participants in the MET37/2b cruise and the crew of FS METEOR for their valuable help. Processing and the modelling work were supported by the MAS3-CT96-60 project of EU. We are very grateful to T. Rellán for the preparation of figures.

References

Anderson, S.A., 1995. On the hydrogen and oxygen contents of marine phytoplankton. Deep-Sea Res. 42, 1675–1680.

Arhan, M.A., King, B., 1995. Lateral mixing of the Mediterranean Water in the eastern North Atlantic. J. Mar. Res. 53, 865–895.

Arhan, M.A., Colin De Verdière, A., Memery, L., 1994. The eastern boundary of the subtropical North Atlantic. J. Phys. Oceanogr. 24 (6), 1295–1316.

Broecker, W.S., 1974. 'NO', a conservative water-mass tracer. Earth Planet. Sci. Lett. 23, 100–107.

Broecker, W.S., Peng, T.H., 1982. Tracers in the Sea. Ed Lamont-Doherty Geological Observatory, New York, 690 pp.

Broecker, W.S., Takahashi, T., 1980. Hydrography of the Central Atlantic: III. The North Atlantic deep-water complex. J. Geophys. Res. 27A, 591–613.

Broenkow, W.W., 1965. The distribution of nutrients in the Costa Rica Dome in the eastern tropical Pacific Ocean. Limnol. Oceanogr. 10, 40–52.

Castro, C.G., Pérez, F.F., Holley, S., Ríos, A.F., 1998. Characterization and modelling of water masses in the Northeast Atlantic. Prog. Oceanogr. 41 (3), 249–279.

Cullen, J.J., Zhu, M., Davis, R.F., Pierson, D.C., 1985. Vertical migration, carbohydrate synthesis and nocturnal nitrate uptake during growth of *Heterocapsa niei* in a laboratory water column. In: Anderson, W.B. (Ed.), Toxic Dinoflagellates. Elsevier, New York, pp. 189–194.

DOE, 1994. In: Dickson, A.G., Goyet, C. (Eds.), Handbook of Methods for the Analysis of the Various Parameters of the Carbon Dioxide System in Sea Water, ORNL/CDIAC-74, SOP 2. 18 pp.

Doney, S., Bullister, J.L., 1992. A chlorofluorocarbon section in the eastern North Atlantic. Deep-Sea Res. 39 (11/12), 1857–1883.

Fiúza, A.F.G., 1984. Hidrologia e dinamica das aguas costeiras de Portugal. PhD Thesis, Univ. Lisbon, 294 pp.

Fraga, F., Pérez, F.F., 1990. Transformaciones entre composición química del fitoplancton, composición elemental y relación de Redfield. Sci. Mar. 54 (1), 69–76.

Fraga, F., Barton, E.D., Llinás, O., 1985. The concentration of nutrient salts in "pure" North and South Atlantic Central Waters. Simp. Int. Afl. Afr., Inst. Inv. Pesq., Barcelona 1, 25–36.

Fraga, F., Ríos, A.F., Pérez, F.F., Figueiras, F.G., 1998. Theoretical limits of oxygen:carbon and oxygen:nitrogen ratios during photosynthesis and mineralisation of organic matter in the sea. Sci. Mar. 62 (1–2), 161–168.

Hansen, H.P., Grasshoff, K., 1983. In: Grasshoff, K. (Ed.), Automated Chemical Analysis in Methods of Seawater Analysis. Verlag-Chemie, Weinheim, pp. 3347–3395.

Harvey, J. et al., 1982. $\theta - S$ relationships and water masses in the eastern North Atlantic. Deep-Sea Res. 29 (8A), 1021–1033.

Harvey, J., Arhan, M., 1988. The water masses of the Central North Atlantic in 1983–84. J. Phys. Oceanogr. 18, 1855–1875.

Johnson, K.M., Wills, K.D., Butler, D.B., Johnson, W.K., Wong, C.S., 1993. Coulometric total carbon dioxide analysis for marine studies: automation and calibration. Mar. Chem. 44, 167–187.

Käse, R.H., Price, J.F., Richardson, P.L., Zenk, W., 1986. A quasi-synoptic survey of the thermocline circulation and water masses distribution within the Canary Basin. J. Geophys. Res. 91 (C8), 9739–9748.

Kawase, M., Sarmiento, J.L., 1986. Circulation and nutrients in mid-depth Atlantic waters. J. Geophys. Res. 91 (C8), 9749–9770.

Lavin, A., Bryden, H.L., Parrilla, G., 1998. Meridional transport and heat flux variations in the subtropical north Atlantic. Global Atmos. Ocean Syst. 6, 269–293.

Laws, E.A., 1991. Photosynthetic quotients, new production and net community production in the open ocean. Deep-Sea Res. 38 (1), 143–167.

Le Groupe CITHER-3, 1998. Recueil de données: Vol. 3. Traceurs Géochimiques. Rapport Interne LPO (98-03), 586 pp.

Le Groupe Tourbillon, 1983. The Tourbillon experiment: a study of mesoscale eddy in the eastern North Atlantic. Deep-Sea Res. 30, 475–511.

Llinás, O., Rodriguez de Leon, A., Siedler, G., Wefer, G., 1997. ESTOC data report. Inf. Tech. Inst. Can. C. Mar., Nu. 3, Telde de Gran Canaria.

Mackas, D.L., Denman, K.D., Bennett, A.F., 1987. Least squares multiple tracer analysis of water mass composition. J. Geophys. Res. 92 (C3), 2907–2918.

Manríquez, M., Fraga, F., 1978. Hidrografía de la región de afloramiento del noroeste de África–Campaña "ATLOR VII". Res. Exp. Cient. B/O Cornide 7, 1–32.

McCartney, M., Talley, T., 1982. The subpolar mode water of the North Atlantic Ocean. J. Phys. Oceanogr. 12, 1169–1188.

Minas, H.J., Packard, T.T., Minas, M., Coste, B., 1982. An analysis of the production–regeneration system in the coastal upwelling area off NW Africa based on oxygen, nitrate and ammonium distributions. J. Mar. Res. 40 (3), 615–641.

Minster, J.-F., Boulahdid, M., 1987. Redfield ratios along isopycnal surfaces—a complementary study. Deep-Sea Res. 34 (12), 1981–2003.

Müller, T.J., Holfort, J., Delahoyde, F., Williams, R., 1995. MKIIIB-CTD: improving its system output. Deep-Sea Res., Part I 42 (11/12), 2113–2126.

Östlund, H.G., Rooth, C.G.H., 1990. The North Atlantic Tritium and radiocarbon transients 1972–1983. J. Geophys. Res. 95 (C11), 20147–20165.

Paillet, J., Mercier, H., 1997. An inverse model of the eastern North Atlantic general circulation and thermocline ventilation. Deep-Sea Res., Part I 44 (8), 1293–1328.

Paillet, J., Arhan, M., McCartney, M.S., 1998. Spreading of Labrador Sea Water in the eastern North Atlantic. J. Geophys. Res. 103 (C5), 10223–10239.

Pérez, F.F., Fraga, F., 1987. The pH measurements in seawater on NBS scale. Mar. Chem. 21, 315–327.

Pérez, F.F., Mouriño, C., Fraga, F., Ríos, A.F., 1993. Displacement of water masses and remineralization rates off the Iberian Peninsula by nutrient anomalies. J. Mar. Res. 51, 1–24.

Pérez, F.F., Ríos, A.F., Castro, C.G., Fraga, F., 1998. Mixing analysis of nutrients, oxygen and dissolved inorganic carbon in the upper and middle North Atlantic ocean east of the Azores. J. Mar. Syst. 16 (3–4), 219–233.

Pollard, R.T., Pu, S., 1985. Structure and circulation of the upper Atlantic Ocean Northeast of the Azores. Prog. Oceanogr. 14, 443–462.

Redfield, A.C., Ketchum, B.H., Richards, F.A., 1963. The influence of organisms on the composition of seawater. The Sea, vol. 2, Wiley, New York, pp. 26–77.

Reid, J.H., 1994. On the total geostrophic circulation of the North Atlantic Ocean: flow patterns, tracers and transports. Prog. Oceanogr. 33, 1–92.

Rhein, M., Hinrichsen, H.H., 1993. Modification of Mediterranean Water in the Gulf of Cadiz, studied with hydrographic, nutrient and chlorofluoromethane data. Deep-Sea Res., Part I 40 (2), 267–291.

Ríos, A.F., Fraga, F., Pérez, F.F., 1989. Estimation of coefficients for the calculation of 'NO', 'PO' and 'CO', starting from the elemental composition of natural phytoplankton. Sci. Mar. 53 (4), 779–784.

Ríos, A.F., Pérez, F.F., Fraga, F., 1992. Water masses in upper and middle North Atlantic Ocean east of the Azores. Deep-Sea Res. 39 (3/4), 645–658.

Ríos, A.F., Anderson, T., Pérez, F.F., 1995. The carbonic system distribution and fluxes in the NE Atlantic during spring 1991. Prog. Oceanogr. 35 (IV), 295–314.

Rios, A.F., Fraga, F., Figueiras, F.G., Pérez, F.F., 1998. A modeling approach to the Redfield ratio deviations in the ocean. Sci. Mar. 62 (1–2), 169–176.

Saunders, P.M., 1986. The accuracy of measurements of salinity, oxygen, and temperature in the deep ocean. J. Phys. Oceanogr. 16, 189–195.

Siedler, G., Kuhl, A., Zenk, W., 1987. The Madeira mode water. J. Phys. Oceanogr. 17, 1561–1570.

Speer, K.G., 1993. The deep silica tongue in the North Atlantic. Deep-Sea Res., Part I 40 (5), 925–936.

Spencer, C.P., 1975. The micronutrient elements. In: Riley, J.P., Skirrow, G. (Eds.), Chemical Oceanography. Academic Press, London, 1087 pp.

Stoll, M.H.C., van Aken, H.M., de Baar, H.J.W., Kraak, M., 1996. Carbon dioxide of water masses in the northern North Atlantic Ocean. Mar. Chem. 55, 217–232.

Stramma, L., Müller, T.J., 1989. Some observations of the Azores Current and the North Ecuatorial current. J. Geophys. Res. 94 (c3), 3181–3186.

Sverdrup, H.U., Johnson, M.W., Fleming, R.H., 1942. The Oceans: Their Physics, Chemistry, and General Biology. Prentice-Hall, Englewood Cliffs, NJ, 1087 pp.

Takahashi, T., Broecker, W.S., Langer, S., 1985. Redfield ratio based on chemical data from isopycnal surfaces. J. Geophys. Res. 90 (C4), 6907–6924.

Talley, L.D., McCartney, M.S., 1982. Distribution and circulation of Labrador Sea Water. J. Phys. Oceanogr. 12, 1189–1205.

Tomczak, J.R., 1981. A multi-parameter extension of temperature/salinity diagram for the analysis of non-isopycnal mixing. Prog. Oceanogr. 10, 147–171.

Tomczak, M., Large, D.G.B., 1989. Optimum multiparameter analysis of mixing in the thermocline of the eastern Indian Ocean. J. Geophys. Res. 94 (C11), 16141–16149.

TTO, 1981. Transient Tracers in the Oceans North Atlantic Study: Vol. 2. Shipboard Physical and Chemical Data Report. Scripps Institution of Oceanography, University of California, San Diego, April 1–October 19.

Tsuchiya, M., 1989. Circulation of the Antarctic Intermediate Water in the North Atlantic Ocean. J. Mar. Res. 47, 747–755.

Tsuchiya, M., Talley, L.D., McCartney, M.S., 1992. An eastern Atlantic section from Iceland southward across the equator. Deep-Sea Res. 39 (11/12), 1885–1917.

UNESCO, 1986. Progress on oceanographic tables and standards 1983–1986, Vol. 50. Work and recommendations of the UNESCO/SCOR/ICES/IAPSO Joint Panel. UNESCO Technical Papers in Marine Science.

van Aken, H.M., 2000a. The hydrography of the mid-latitude northeast Atlantic Ocean: the deep water masses. Deep-Sea Res. 47 (5), 757–788.

van Aken, H.M., 2000b. The hydrography of the mid-latitude northeast Atlantic Ocean: the intermediate water masses. Deep-Sea Res. 47 (5), 789–824.

Villarreal, T.A., Pilskaln, C., Brzezinski, M., Lipschultz, F., Dennett, M., Gardner, G.B., 1999. Upward transport of oceanic nitrate by migrating diatom mats. Nature 397, 423–425.

Willenbrink, E., 1982. Wassermassenanalyse im tropischen und subtropischen Nordostatlantik. Ber. Inst. Meereskd., Kiel, 96, 72 pp.

WOCE, 1994. WOCE Operations Manual: Vol. 3, Sect. 3.1, Part 3.1.3: WHP Operations and Methods (Oxygen determination). Rev. 1, Nov. 1994. Woods Hole, MA, USA, 12 pp.

Wüst, G., Defant, A., 1936. Atlas zur Schichtung und Zirkulation des Atlantischen Ozeans. Schnitte und Karten von Temperatur, Salzgehalt und Dichte. Wissenschaftliche Ergebnisse der Deutschen Atlantischen Expedition auf dem Forschungs-und Vermessungsschiff “Meteor” 1925–1927. six Atlas, 103 plates.